

Scanning Acoustic Microscopy for Mapping the Microelastic Properties of Human Corneal Tissue

Itthar M. Beshtawi¹, Riaz Akhtar², M Chantal Hillarby³, Clare O'Donnell⁴, Xuegen Zhao⁵, Arun Brahma⁶, Fiona Carley⁶, Brian Derby⁵, and Hema Radhakrishnan¹

¹Carys Bannister Building, Faculty of Life Sciences, The University of Manchester, Manchester, UK, ²Centre for Materials and Structures, School of Engineering, University of Liverpool, Liverpool, UK, ³Institute of Human Development, University of Manchester, Manchester, UK, ⁴Optegra Eye Sciences, Optegra Manchester Eye Hospital, Optegra, One Didsbury Point, Didsbury, Manchester, UK, ⁵Manchester Materials Science Centre, School of Materials, The University of Manchester, Manchester, UK, and ⁶Manchester Royal Eye Hospital, Manchester, UK

ABSTRACT

Purpose: To assess the feasibility of applying scanning acoustic microscopy (SAM) on UV cross-linked corneal tissue for mapping and analyzing its biomechanical properties.

Materials and Methods: Five corneal pairs (10 corneas) were used. In each pair, one cornea was cross-linked (epithelium removed, riboflavin application for 45 min and UVA irradiation for 30 min) and the contralateral control cornea was epithelial debrided and treated only with riboflavin for 45 min. Histological sections were prepared and their mechanical properties were examined using SAM. A line profile technique and 2D analysis was used to analyze the mechanical properties of the corneas. Then the corneal paraformaldehyde and unfixed sections were examined histologically using hematoxylin and eosin (H&E) staining.

Results: In the frozen fresh corneal tissue, the speed of sound of the treated corneas was $1672.5 \pm 36.9 \text{ ms}^{-1}$, while it was $1584.2 \pm 25.9 \text{ ms}^{-1}$ in the untreated corneas. In the paraformaldehyde fixed corneal tissue, the speed of sound of the treated corneas was $1863.0 \pm 12.7 \text{ ms}^{-1}$, while it was $1739.5 \pm 30.4 \text{ ms}^{-1}$ in the untreated corneas. The images obtained from the SAM technique corresponded well with the histological images obtained with H&E staining.

Conclusion: SAM is a novel tool for examining corneal tissue with a high spatial resolution, providing both histological and mechanical data.

Keywords: Biomechanics, cross-linking, human cornea, riboflavin, scanning acoustic microscopy

INTRODUCTION

Cornea is a viscoelastic tissue,¹ composed of collagen and elastic fibres.^{2,3} The elasticity of the corneal tissue changes with age^{4,5} and in cases of ocular pathology such as keratoconus.^{6–8} Corneal collagen cross-linking has emerged as a new treatment for keratoconus in the past decade.^{9–12} Its principle is based on strengthening the corneal surface by enhancing the chemical bonds within collagen fibres^{11,12} and within the matrix between them.¹³ The recent interest in assessing the effects of collagen cross-linking on corneal tissue has increased the necessity of developing and using

reliable and accurate techniques for measuring the corneal biomechanical properties. Different methodologies have been used to assess the bulk biomechanical properties of the cornea, such as strip extensometry and inflation. We assess the possibility of using scanning acoustic microscopy (SAM) to map the mechanical properties of corneal tissue pixel by pixel (with a spatial resolution of $1 \mu\text{m}$).

SAM is a non-destructive imaging technique that can be used to analyze the structural properties of materials point by point, allowing both qualitative and quantitative characterization of the tissue.^{14–17} SAM can provide information about sample

Received 16 September 2012; revised 13 November 2012; accepted 21 November 2012; published online 7 February 2013

Correspondence: Hema Radhakrishnan, PhD, Faculty of Life Sciences, Carys Bannister Building, The University of Manchester, Dover Street, Manchester, M13 9PL, UK. Fax: 01613063887. E-mail: Hema.Radhakrishnan@manchester.ac.uk

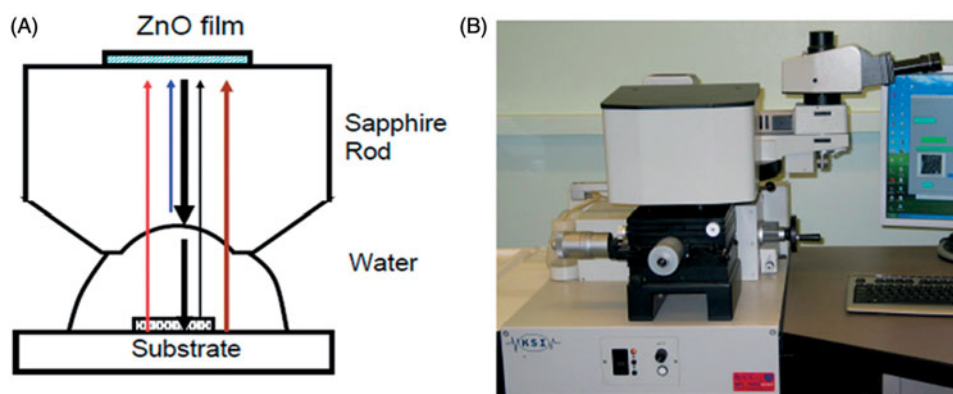


FIGURE 1. A schematic operation of SAM: (A) the transducer generates an acoustic pulse which propagates through the coupling fluid. When a sound wave is generated and propagates through the acoustic lens, medium and specimen there are reflections from acoustic lens/medium, specimen/medium, specimen/substrate and medium/substrate interfaces. The contrast observed in a SAM image contains complex phase information from the recombination of these signals. The transducer and lens correspond to ZnO film and sapphire rod, respectively. (B) SAM 2000 instrument utilized in this study.

thickness, density, attenuation, roughness and stiffness.¹⁸ Further, as the technique uses high-frequency ultrasound (100 MHz–1 GHz), a high spatial resolution can be achieved (around 1 μ m at 1 GHz).

Although SAM is most widely used in the microelectronics and metallurgy industries,¹⁸ the technique has long been recognized as a powerful tool for biomedical application.¹⁹ It has been used to characterize hard tissues such as bones and teeth,^{20–22} living cells²³ and soft tissues such as blood vessels^{24,25} and heart valves.²⁶ The attractiveness of SAM for biomedical applications is the ease of sample preparation, the ability to obtain histological information alongside the mechanical property data and its non-destructive nature.

The principle of SAM is based on using ultrasound waves which can propagate within the sample^{14,17}, Figure 1. The acoustic waves are transmitted through a coupling fluid, usually distilled water.^{14,15} The requirement for a coupling fluid is advantageous for biological samples as it means they are kept hydrated during testing.

The key component of SAM is a piezoelectric transducer which is responsible for transmitting and receiving the acoustic waves.¹⁵ The transducer transforms the electrical signals into acoustic waves which then propagate through the coupling fluid. A lens is used to focus the acoustic waves on the surface of the sample and the waves reflected back from the sample are analyzed.¹⁵ The lens is scanned horizontally in the x - and y -directions by a pair of oscillator coil drivers to produce C-mode two-dimensional (2-D) images. The SAM instrument has a z -stage that allows the lens–sample distance to vary.

For engineering materials, quantitative data are obtained from SAM images using the $V(z)$ -method (recording of output voltage versus defocus distance, z) which determines the velocity of surface acoustic waves (Rayleigh waves). However, this technique is not suitable for soft biological specimens because it

requires a very smooth specimen surface and also because Rayleigh waves are rapidly attenuated in biological tissues.¹⁶ A number of approaches have been developed to obtain quantitative data for biological tissues and cells including a recently developed phase analysis method.²⁷ The aim of this study is to investigate the feasibility of applying SAM technique on corneal tissue.

MATERIALS AND METHODS

Five human corneal pairs (three males, two females) were obtained from Manchester Eye Bank and included in this study. The age range of the corneal samples was 54–86 years. These corneas were contra-indicated for corneal transplantation (for causes which did not involve the eye directly e.g. insufficient medical history). All the corneas had research permission from the donors' relatives if transplantation was not possible.

The corneas with a 3 mm scleral rim were removed from the eyes within 24 h of death and placed in organ culture media at 34 °C. During this period the corneas swell due to changes in the extracellular matrix. After 10 days the corneas were assessed macroscopically for the presence of opacities and scars and microscopically for the quality of endothelium (determined from the endothelial cell counts). After the cell count, the corneas were placed in fresh media containing 10% dextran and incubated at 34 °C for a further 24 h to allow the corneas to shrink back to normal thickness.

In each pair, one cornea was cross-linked (epithelium removed, riboflavin 0.1% solution (10 mg riboflavin-5-phosphate in 20% dextran-T-500 10 mL solution) application for 15–30 min prior to UV-A irradiation (370 nm, 3 mW/cm²) for 30 min using VEGA CBM X-LINKER[®] (CSO, Florence, Italy), while the riboflavin was being applied), and the contralateral cornea was exposed to riboflavin only without UV-A exposure and served as a control.

Three corneal pairs were embedded in OCT™ (Tissue-Tek, CellPath, Powys, UK) and the central part was sectioned using a cryostat to a thickness of 5 µm. Then, the sections were mounted on clean glass slides, air dried and stored at -80 °C until usage. Furthermore, two corneal pairs were fixed in Paraformaldehyde (4%) for 24 hours then embedded in paraffin wax and subsequently stored at -20 °C for 24 h. Once the corneas were set in the paraffin blocks, 5 µm thick sections were obtained from the central part of the cornea. Then, the samples were mounted on glass slides, incubated at 37 °C overnight and rehydrated through xylene and a series of graded alcohols. Corneal sections were imaged by SAM and then stained by hematoxylin and eosin (H&E). Corneal sections were taken from the central part of the frozen-fresh and paraffin-fixed corneas and the first 200 × 200 µm area of each section was imaged and analyzed by SAM and then stained by H&E according to a standard procedure.

Principles of SAM

We have described the principles of SAM in detail elsewhere.²⁷ In brief, the SAM instrument utilizes a pulse of high-frequency acoustic waves (typically 100 MHz–1 GHz) which is transmitted from an acoustic lens, through a coupling fluid (either water or a buffered saline solution) to the sample. The reflected signal is the result of interference between the reflected acoustic signal and any retransmission from surface acoustic waves. This generates contrast that varies periodically with defocus. In stiff materials, this can be analyzed to determine elastic constants of the material. In soft biological tissues, quantitative analysis is more challenging. When a thin biological specimen is mounted on a glass substrate and immersed in an acoustic coupling fluid (such as distilled water or buffered saline), reflections are generated at each interface in the system: lens/fluid, fluid/specimen and specimen/substrate. In addition Rayleigh waves may radiate along the substrate surface and these leaky Rayleigh waves radiate acoustic energy from the substrate toward the lens. The signal received at the lens thus results from the interference between the reflections and the amplitude determined by the intensities and phase of each wave. We have developed a new method, multi-layer phase analysis (MLPA)²⁷, which utilizes phase information that is preserved in the interference that occurs between the acoustic wave reflected from the substrate surface and internal reflections from the acoustic lens, to extract quantitative data from SAM images. The spatial resolution is a function of the wavelength of the acoustic radiation; with a 1 GHz acoustic signal, the spatial resolution achievable is close to 1 µm.

The speed of sound (c) determined by SAM is related to the tissue properties by the following equation:

$$c = \sqrt{\frac{E(1-\nu)}{\rho(1+\nu)(1-2\nu)}} \quad (1)$$

where E is Young's modulus, ν is Poisson's ratio and ρ is the density of the material. The equation demonstrates that Young's modulus is directly proportional to the square value of the speed of sound measured with SAM.

SAM Imaging with MLPA

SAM imaging was conducted with a SAM 2000 microscope (PVA TePla Analytical Systems GmbH, Herborn, Germany) modified with a custom data acquisition and control system.²⁷ The SAM images were acquired using MATSAM software (Julius Wolff Institut & Berlin-Brandenburg School for Regenerative Therapies, Berlin, Germany) and the method MLPA.²⁷ In brief, with the MLPA method, the acoustic focal point of the lens is initially set 4 µm above substrate surface. A series of 200 × 200 µm C-scan images are then taken at different z -positions starting from this height toward the substrate surface with a step-size of 0.1 µm over a range of 5 µm. For this study, the images were acquired at 761 MHz which was found to be the optimal acoustic frequency for the cornea samples. Distilled water was used as the coupling fluid and the experiments were conducted at room temperature.

The images were processed off-line with custom software using the phase analysis method developed by Zhao et al.²⁷ In summary, the gray scale value for every pixel (x, y position) was extracted from every image at each z position to form a $V(z)$ curve. The $V(z)$ data were then filtered and processed by Fast Fourier Transformation. A 2D phase array is then obtained for the dataset which is then processed and converted to a speed of sound map as shown in Figure 2.

Histology

After SAM imaging, the corneal sections were stained with H&E following a standard procedure. Slides with paraffin fixed corneal tissue sections were first de-waxed for two minutes in 95%, 90%, 80% and 70% xylene, and then they were immersed for two minutes in four different pots of industrial methylated spirit (IMS) to remove xylene and placed in tap water for two minutes. Then they were kept in filtered hematoxylin (Shandon Harris Haematoxylin, Thermo Scientific, Cheshire, UK) for only a minute and were then immediately immersed in tap water.

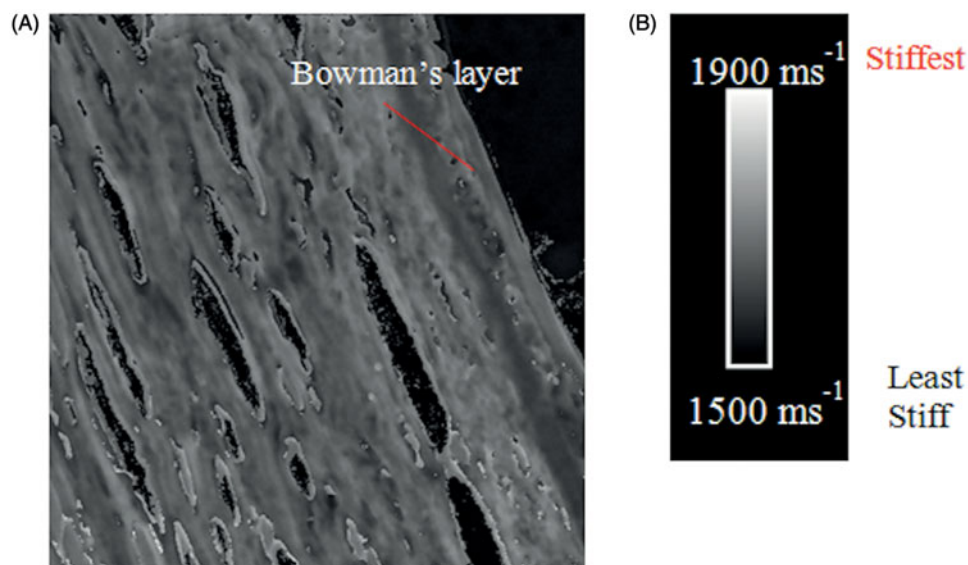


FIGURE 2. Speed of sound (stiffness) map for corneal section (A) and the brightest regions representing the stiffest components of the tissue section (B).

The following steps were followed: dipping the slides twice in acid alcohol, and keeping them under running warm tap water for five minutes. The slides were then kept in alcoholic eosin (Shandon Eosin Y Alcoholic, Thermo Scientific, Cheshire, UK) for half a minute, dipped quickly through the four IMS pots and then dipped through the 95%, 90%, 80% and 70% xylene pots, for a minute each. Finally, the slides were mounted by using transparent coverslips and DPX mounting (Shandon Consul-Mount™, Thermo Scientific, Cheshire, UK), and then the slides were left to air-dry for 20 min. The same procedure was applied to the frozen corneal sections, but without de-waxing in xylene. The stained sections were then visualized by optical microscopy (Leica LEITZ DMRB microscope, San Jose, CA) and the images were captured using an INFINITY-X digital camera and DeltaPix software.

RESULTS

Figure 3 illustrates corneal cross-sections ($200 \times 200 \mu\text{m}$) imaged first by SAM (A, C, E, G) and then subsequently stained with H&E and imaged with the optical microscope (B, D, F, H). The cross-linked corneal sections (A, E) showed brighter images than the untreated cornea tissue sections (C, G). The same level of histological detail is visible in both sets of images although the former images were acquired without any staining. Furthermore, gaps are visible in both imaging techniques, which are the artifacts created as a result of the sectioning process.

The SAM images can be analyzed either by taking measurements across a line profile (Figure 4) or by averaging the values within a region of the cornea

(Figure 5). The analysis automatically excludes the air pockets and artificial tears. Figure 4 shows the local variation in stiffness across the line profile. Such information cannot be gleaned from techniques where global measurements are obtained, for example, from an entire corneal strip.

In this study, we used both a line profile technique and 2D analysis to analyze the intrinsic properties of the cross-linked and untreated corneas in the anterior $200 \times 200 \mu\text{m}$ of the corneal tissue.

In the frozen fresh corneal tissue, the speed of sound, which is related to the tissue stiffness, was $1672.5 \pm 36.9 \text{ ms}^{-1}$ while it was $1584.2 \pm 25.9 \text{ ms}^{-1}$ in the untreated corneas (which gives 1.056 increase factor). In the paraformaldehyde fixed corneal tissue, the speed of sound of the treated corneas was $1863.0 \pm 12.7 \text{ ms}^{-1}$, while it was $1739.5 \pm 30.4 \text{ ms}^{-1}$ in the untreated corneas (which gives 1.071 increase factor).

The posterior $200 \times 200 \mu\text{m}$ regions of the cross-linked and untreated frozen corneas were also imaged using the scanning acoustic microscope (Figure 6). The speed of sound of the posterior portion of the cross-linked corneas was $1591.4 \pm 20.0 \text{ ms}^{-1}$ while it was $1557.7 \pm 19.7 \text{ ms}^{-1}$ in the untreated corneas (which gives 1.050 increase factor between the anterior and posterior portions of the cross-linked cornea).

DISCUSSION

In vitro measurement of corneal stiffness and other mechanical properties is important to understand the mechanisms of corneal pathology and to assess the effectiveness of different types of treatments.

We chose to explore the feasibility of applying quantitative SAM to determine the elastic properties

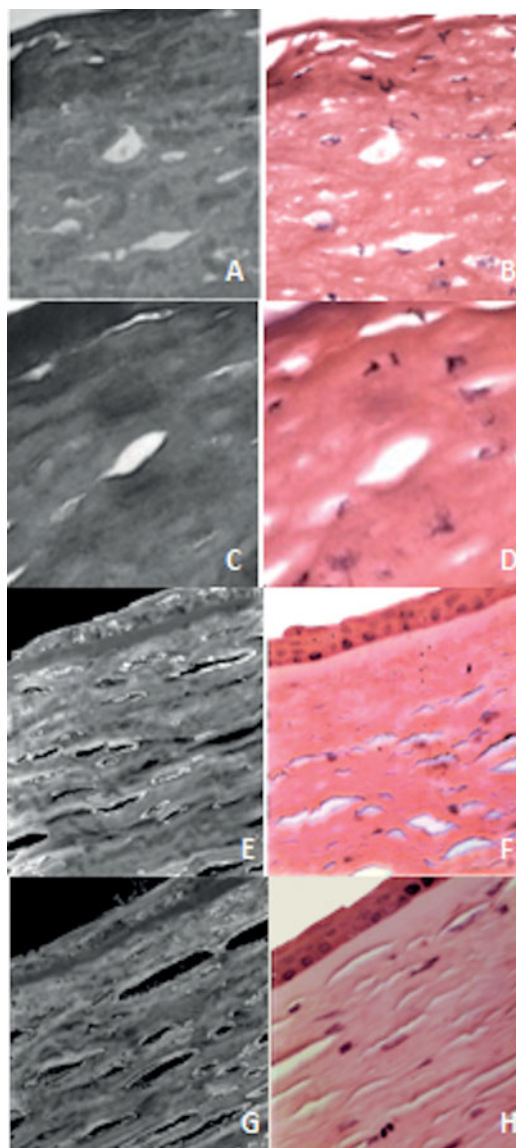


FIGURE 3. Frozen fresh (A, B, C, D) and paraffin fixed (E, F, G, H) cornea tissue sections imaged by SAM (A, C, E, G) and then by optical microscopy (B, D, F, H) following H&E staining. Brighter images were obtained from the cross-linked cornea tissue sections (A, E), when compared with sections taken from the untreated corneas (C, G). Each image is $200 \times 200 \mu\text{m}$. In each pair of images the same SAM section has been stained for optical microscopy following SAM imaging; however, the pair of images has not been registered.

of corneal tissue because it is a relatively fast technique, requires minimal sample preparation and provides a high spatial resolution. Corneal tissue stiffness can be determined for every pixel in the SAM images, and thus gives precise mechanical property information across the different layers of the cornea. Moreover, artificial gaps in the tissue section can be excluded from the analysis (Figure 5). It is also a non-destructive technique and thus the samples can be used for subsequent measurements with other techniques, e.g. immunohistochemistry.

The most commonly used method to assess the mechanical properties of corneal tissue is the strip

extensometry technique due to its simplicity.^{12,28,29} However, this technique results in the stromal lamellae being cut.³⁰ Additionally, the accuracy and the reliability of this method are variable for some reasons. Firstly, the strip extensometry technique flattens the strips taken from the corneas, as they are naturally curved.³⁰ Secondly, it neglects the variation in the length of the centerline and edges of the corneal strip and it also neglects the thickness variation between the corneal center and periphery.³⁰ Furthermore, only one strip can be taken from each cornea and thus only one measurement can be made per section. In contrast, as only thin sections are used for SAM, multiple sections can be imaged per cornea. Nonetheless, on average, the SAM technique, in this study, and strip extensometry from previous studies found an increase rigidity of the cross-linked corneas when compared with the untreated corneas.

In this study, SAM images taken from the cross-linked corneas (Figure 3A and E) were found to be brighter than the untreated corneal tissue sections (Figure 3C and G), which reflect a higher speed of sound and a higher stiffness in the cross-linked corneas in both the frozen fresh and the paraformaldehyde fixed tissue. The speed of sound measurements in both fixation methods showed an increase in stiffness by a factor of $1.056\times$ and 1.071 , respectively, between the cross-linked and the untreated corneas using the SAM technique. A higher speed of sound was found in the anterior part of the cross-linked corneas than in the posterior part of the same sample ($1.05\times$) which indicates that the cross-linking effect is mainly concentrated in the anterior part of the cornea. However, the speed of sound values were found to be higher in the paraffin fixed tissue, which may be due to the paraffin fixing procedure. The cryosections are more representative of the intrinsic stiffness of the cornea.

The increase in stiffness between the cross-linked and untreated corneal tissue ($1.1\times$) is a bit lower than what was reported by previous studies. The increase in Young's modulus after cross-linking was found to be by a factor of $1.3\times$ three months after treatment³¹ and by $1.5\times$ immediately after treatment.³² Similar results were reported by Spoerl et al.¹² ($1.5\times$) and by Lanchares et al.²⁹ ($1.6\times$). Moreover, our value matches very well with what was reported by Kohlhaas et al.²⁸ for the anterior portion of the cornea. In the Kohlhaas et al.²⁸ study, two anterior and posterior flaps of $200 \mu\text{m}$ thickness were cut from the corneas and Young's modulus was calculated separately for each flap. An increase by a factor of 1.66 was reported from the anterior flaps, which matches the increase of sound speed in the anterior $200 \mu\text{m}$ thickness analysis in our study using SAM.

Another advantageous feature of SAM is that the images provide both histological and mechanical property data. The histological features visible in the

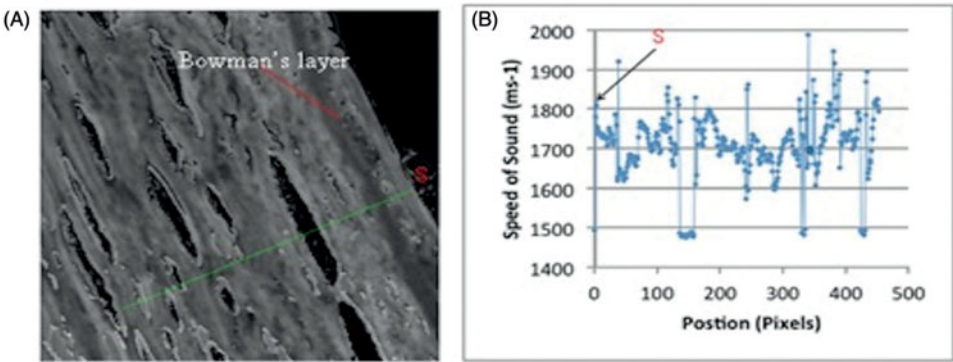


FIGURE 4. (A) Line profile through cornea section showing pixel by pixel variation in stiffness across the different layers of the corneal section and (B) the line begins close to glass substrate (S), traverses Bowman's layer and then deeper into the cornea.

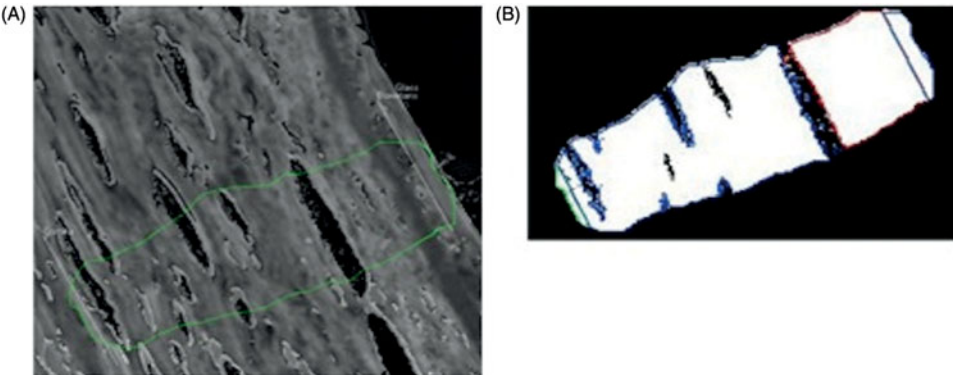


FIGURE 5. (A) Region selected for 2-D analysis and (B) only the regions that appear white in the inset image are analyzed (artificial tears in the tissue are automatically excluded from the analysis).

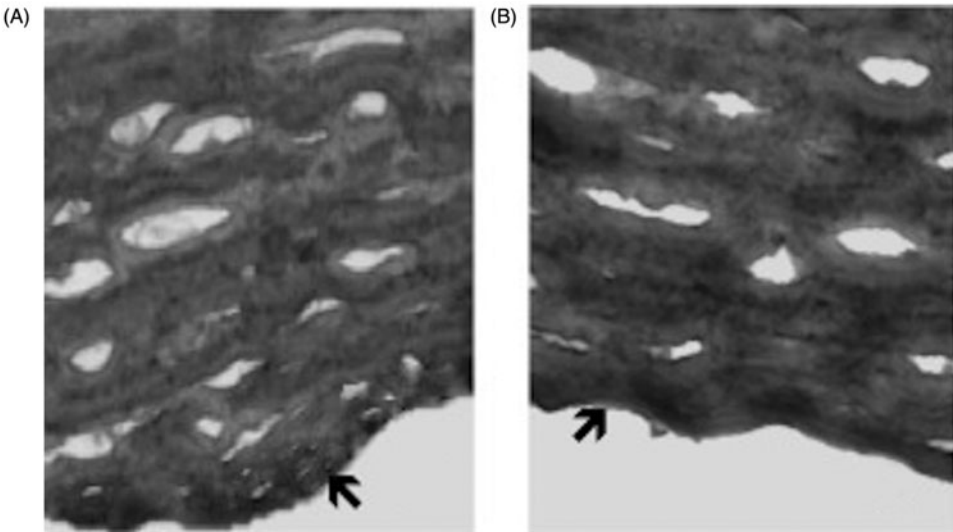


FIGURE 6. The posterior (200 × 200) μm portion of cross-linked (A) and untreated (B) frozen cornea tissue sections imaged by SAM. Arrows refer to the corneal endothelium.

optical images following H&E staining are clearly visible in the SAM image without any staining (Figure 3). Coupled with the high spatial resolution quantitative data that are obtained, SAM becomes a powerful tool for studying changes within corneal tissue.

Akhtar *et al.*¹⁶ compared images of ferret aorta obtained from the same section which was first imaged with SAM at 400 MHz and subsequently stained with H&E and then imaged with fluorescence microscopy. A similar spatial resolution was achieved in both images, with the elastic fibers clearly visible in

the SAM images without any fixation or staining. More recently, Graham et al.³³ have shown that at 1 GHz, SAM images of ovine aorta encompass both elastin-rich lamellae and fibrillar collagen, which can be clearly identified by subsequent fluorescence microscopy (elastin autofluorescence) and polarized light microscopy (following picrosirius red stain for collagen).

The vast majority of studies on SAM, similar to this investigation, have been conducted with chemically fixed sections as utilized in this study (e.g. Saijo et al.³⁴). However, we also used unfixed cryosections in order to avoid inducing any mechanical changes in the tissues due to the fixation process¹⁶. The results from the cryosectioned corneal samples were found to be similar to those in fixed samples when comparing the cross-linked versus un-crosslinked corneal tissue. However, the speed of sound varied between fixed and unfixed samples. To avoid artifacts caused by inadequate de-waxing or changes in corneal structure due to the fixing procedure, it might be useful to apply the SAM technique to cornea cryosections only for future investigations.

In conclusion, SAM can be used to effectively determine the mechanical properties of corneal tissue qualitatively and quantitatively. It can be used to determine the intrinsic properties of corneal tissue and detect the variation of the speed of sound between cross-linked and untreated corneas. The increase in the speed of sound of the anterior 200 µm using SAM matches well with strip extensometry for the anterior portion of the cornea.

ACKNOWLEDGEMENTS

The authors thank Mr Isaac Zambrano and the Manchester Eye Bank for providing the corneas for this study, and Dr Sebastian Brand (Fraunhofer Institute of Material Mechanics, Germany) and Prof. Kay Raum (Julius Wolff Institut & Berlin-Brandenburg School for Regenerative Therapies, Germany) who developed the MATSAM software utilized in this study.

DECLARATION OF INTEREST

Development of the SAM was funded by Wellcome Trust (WT085981AIA). I.B.'s PhD is funded by An-Najah National University, Nablus, Palestine.

REFERENCES

1. Luce DA. Determining in vivo biomechanical properties of the cornea with an ocular response analyzer. *J Cataract Refract Surg* 2005;31:156–162.
2. Nakayasu K, Tanaka M, Konomi H, et al. Distribution of types I, II, III, IV and V collagen in normal and keratoconus corneas. *Ophthalmic Res* 1986;18:1–10.
3. Meisenberg G, Simmons WH. Principles of medical biochemistry. St Louis (MO): Mosby Co.; 2006.
4. Daxer A, Misof K, Grabner B, et al. Collagen fibrils in the human corneal stroma: structure and aging. *Invest Ophthalmol Vis Sci* 1998;39:644–648.
5. Elsheikh A, Wang DF, Brown M, et al. Assessment of corneal biomechanical properties and their variation with age. *Curr Eye Res* 2007;32:11–19.
6. Kirwan C, O'Malley D, O'Keefe M. Corneal hysteresis and corneal resistance factor in keratoectasia: findings using the Reichert Ocular Response Analyzer. *Ophthalmologica* 2008;222:334–337.
7. Touboul D, Roberts C, Kerautret J, et al. Correlation between corneal hysteresis intraocular pressure, and corneal central pachymetry. *J Cataract Refract Surg* 2008;34:616–622.
8. Ambekar R, Toussaint KC, Johnson AW. The effect of keratoconus on the structural, mechanical, and optical properties of the cornea. *J Mech Behav Biomed Mater* 2011;4:223–236.
9. Wollensak G, Spoerl E, Seiler T. Riboflavin/ultraviolet-A-induced collagen crosslinking for the treatment of keratoconus. *Am J Ophthalmol* 2003;135:620–627.
10. Wollensak G, Spoerl E, Seiler T. Stress-strain measurements of human and porcine corneas after riboflavin-ultraviolet-A-induced cross-linking. *J Cataract Refract Surg* 2003;29:1780–1785.
11. Wollensak G. Crosslinking treatment of progressive keratoconus: new hope. *Curr Opin Ophthalmol* 2006;17:356–360.
12. Spoerl E, Huhle M, Seiler T. Induction of cross-links in corneal tissue. *Exp Eye Res* 1998;66:97–103.
13. Brummer G, Littlechild S, McCall S, et al. The role of nonenzymatic glycation and carbonyls in collagen cross-linking for the treatment of keratoconus. *Invest Ophthalmol Vis Sci* 2011;52:6363–6369.
14. Briggs A. An introduction to scanning acoustic microscopy. Oxford University Press: Oxford University Press; 1985.
15. Da Fonseca RJM, Ferdjallah L, Despau G, et al. Scanning acoustic microscopy – recent applications in materials science. *Adv Mater* 1993;5:508–519.
16. Akhtar R, Sherratt MJ, Watson RE, et al. Mapping the micromechanical properties of cryo-sectioned aortic tissue with scanning acoustic microscopy. *Mater Res Soc Symp Proc* 2009;1132E:Z1103–Z1107.
17. Briggs A, Kolosov O. Acoustic microscopy. 2nd ed. Oxford: Oxford University Press; 2010.
18. Khuriyakub BT. Scanning acoustic microscopy. *Ultrasonics* 1993;31:361–372.
19. Daft CMW, Briggs GAD. The elastic microstructure of various tissues. *J Acoust Soc Am* 1989;85:416–422.
20. Hasegawa K, Turner CH, Recker RR, et al. Elastic properties of osteoporotic bone measured by scanning acoustic microscopy. *Bone* 1995;16:85–90.
21. Eckardt I, Hein HJ. Quantitative measurements of the mechanical properties of human bone tissues by scanning acoustic microscopy. *Ann Biomed Eng* 2001;29:1043–1047.
22. Raum K, Kempf K, Hein HJ, et al. Preservation of microelastic properties of dentin and tooth enamel in vitro – a scanning acoustic microscopy study. *Dent Mater* 2007;23:1221–1228.
23. Kundu T, Bereiter-Hahn J, Karl I. Cell property determination from the acoustic microscope generated voltage versus frequency curves. *Biophys J* 2000;78:2270–2279.

24. Saijo Y, Ohashi T, Sasaki H, et al. Application of scanning acoustic microscopy for assessing stress distribution in atherosclerotic plaque. *Ann Biomed Eng* 2001;29:1048–1053.
25. Saijo Y, Jorgensen CS, Mondek P, et al. Acoustic inhomogeneity of carotid arterial plaques determined by GHz frequency range acoustic microscopy. *Ultrasound Med Biol* 2002;28:933–937.
26. Jensen AS, Baandrup U, Hasenkam JM, et al. Distribution of the microelastic properties within the human anterior mitral leaflet. *Ultrasound Med Biol* 2006;32:1943–1948.
27. Zhao XG, Akhtar R, Nijenhuis N, et al. Multi-layer phase analysis: quantifying the elastic properties of soft tissues and live cells with ultra-high-frequency scanning acoustic microscopy. *IEEE Trans Ultrason Ferroelectr Freq Control* 2012;59:610–620.
28. Kohlhaas M, Spoerl E, Schilde T, et al. Biomechanical evidence of the distribution of cross-links in corneas treated with riboflavin and ultraviolet A light. *J Cataract Refract Surg* 2006;32:279–283.
29. Lanchares E, del Buey MA, Cristobal JA, et al. Biomechanical property analysis after corneal collagen cross-linking in relation to ultraviolet A irradiation time. *Graefes Arch Clin Exp Ophthalmol* 2011;249:1223–1227.
30. Ahearne M, Yang Y, Then KY, et al. Non-destructive mechanical characterisation of UVA/riboflavin crosslinked collagen hydrogels. *Br J Ophthalmol* 2008;92:268–271.
31. Sporl E, Schreiber J, Hellmund K, et al. Studies on the stabilization of the cornea in rabbits. *Ophthalmologe* 2000;97:203–206.
32. McCall AS, Kraft S, Edelhauser HF, et al. Mechanisms of corneal tissue cross-linking in response to treatment with topical riboflavin and long-wavelength ultraviolet radiation (UVA). *Invest Ophth Vis Sci* 2010;51:129–138.
33. Graham HK, Akhtar R, Kridiotis C, et al. Localised micro-mechanical stiffening in the ageing aorta. *Mech Ageing Dev* 2011;132:459–467.
34. Saijo Y, Miyakawa T, Sasaki H, et al. Acoustic properties of aortic aneurysm obtained with scanning acoustic microscopy. *Ultrasonics* 2004;42:695–698.